# A NEARLY 1-D NON-PREMIXED FLAME NEAR EXTINCTION. CELL FORMATION AND THE EFFECT OF THE DIRECTION OF BULK FLOW.

<u>David Lo Jacono</u><sup>1</sup>, Paul Papas<sup>1</sup>, Moshe Matalon<sup>2</sup>, Peter A. Monkewitz<sup>1</sup>

<sup>1</sup> Fluid Mechanics Laboratory, Swiss Federal Institute of Technology Lausanne, Switzerland

<sup>2</sup> McCormick School of Engineering and Applied Sciences, Northwestern University, Evanston, U.S.A.

#### EXPERIMENTAL REALIZATION OF A NEW 1-D FLAME FACILITY

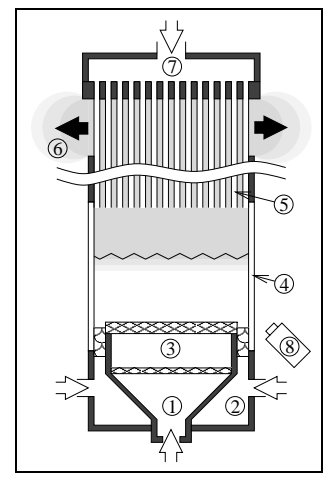


Figure 1. Schematic of the burner. (1) bottom reactant flow, (2) inert co-flow, (3) porous plates, (4) fused silica windows, (5) tube array for reactant supply from top, (6) hot product exhaust, (7) top reactant flow, (8) movie camera.

The *unstrained* one-dimensional diffusion flame has often served as an idealized construct for theoretical modelling [1, 2, 3]. The idealized burner in these studies is supplied with one reactant from the bottom through a "semi-permeable plate" (impermeable in the downward direction). The other reactant diffuses from the top of the chamber to the flame, against the upward flow of products. The supply of both reactants is assumed to be uniform over the burner cross section such that the velocity, which is upwards everywhere, and all other physical quantities depend only on the (vertical) coordinate normal to the planar flame. Since the uniform supply of the reactant diffusing against the bulk flow is a major experimental problem, laboratory investigations of non-premixed flames have until now been limited to burners with non-uniform conditions over the flame surface.

In order to more directly compare the theoretical results for the 1-D ideal flame with experiments, a new improved experimental realization of the ideal burner has been constructed. It is shown schematically in Fig. 1 on which the various components are identified. The combustion chamber with a square cross section of  $46\times46$  mm has a solid back wall with igniter and three fused silica windows. The bottom reactant is introduced into the combustion chamber through a 34 mm square porous plate surrounded by a slot allowing the introduction of an inert co-flow (not used here). In order to obtain a uniform distribution of the top reactant over the cross section, while also allowing the products to escape uniformly, the top reactant is supplied through a cartesian array of  $25\times25$  stainless steel tubes (1 mm O.D., 0.8 mm I.D.) between which the products can escape upwards. Just below the ends of the tubes (located 20 mm above the bottom porous plate), the flow is clearly 3-D on the scale of the tube spacing. Some simple estimates suggest however that the thickness of this 3-D layer is of the order of one tube diameter, and that below this injection region the oxidizer is transported towards the flame by 1-D diffusion against the product flow, as in the ideal burner.

## INVESTIGATION OF EXTINCTION LIMITS AND CELL FORMATION IN THE NEW BURNER

Previous experimental investigations on cell formation in non-premixed flames include the work of Chen et al. [4] who clearly demonstrated that low Lewis and Damköhler numbers are required for cells formation. More recently, the influence of the initial mixture strength on cell formation in an axisymmetric jet flame has been documented at EPFL [5, 6]. While these studies qualitatively confirm the influence of the different parameters predicted theoretically for an ideal 1-D flame, the new burner described above should permit quantitative comparisons. In the following, preliminary results with the new burner are reported for  $CO_2$ -diluted  $H_2$ - $O_2$  nearly unstrained, non-premixed flames near extinction. Two configurations are considered: One with the fuel supplied from the bottom (FB) and the oxidizer counterdiffusing from the top, and the configuration with inverted supplies, i.e. the fuel counterdiffusing from the top (FT). Note that the FB configuration is analogous to the steady axisymmetric jet flame, where the radial bulk flow through the flame is directed outwards from the fuel to the oxidizer side. The same situation is also found in a "lean" flamelet. Finally, for opposed jet flames with highly diluted fuel (e.g.  $N_2$ -diluted  $CH_4$  burning with pure  $O_2$  [7]), the flame sits on the fuel side of the stagnation plane and  $O_2$  reaches the flame by counterdiffusion, again as in the FB configuration.

First, the extinction limit for the FB and FT configurations were determined as a function of the initial  $O_2$  and  $H_2$  concentrations. For this, the top reactant composition was held constant, while the bottom reactant concentration was gradually decreased in small steps until the flame could barely be maintained (a further 0.1% reduction of the bottom reactant concentration below this "near-extinction" limit always resulted in complete extinction). As shown in Fig. 2, these extinction curves have asymptotes corresponding to limiting  $H_2$  and  $H_2$  concentrations, below which a diffusion flame cannot be established, irrespective of how "rich" the other reactant is. The influence of the direction of bulk flow on the limiting  $H_2$  concentration is evident: when  $H_2$  is supplied convectively by the bulk flow (FT configuration), a flame with excess fuel supply can be sustained at about  $H_2$  concentration than in the FB configuration, where  $H_2$  has to diffuse against the bulk flow. The comparison of the limiting  $H_2$  concentrations, on the other hand, has not yet been carried out. Furthermore, it is noted that all the limiting concentrations in Fig. 2 are significantly lower than in the axisymmetric jet flame [5], which is believed to be at least partly due to the negligible flow strain rate in the present

burner. Other effects, such as heat loss, remain to be investigated: for any given reactant composition, the flowrate of the bottom reactant had to be limited keep the flame away from the upper injection manifold. The limit where heat loss to this manifold affects the extinction limits, however, remains to be determined.

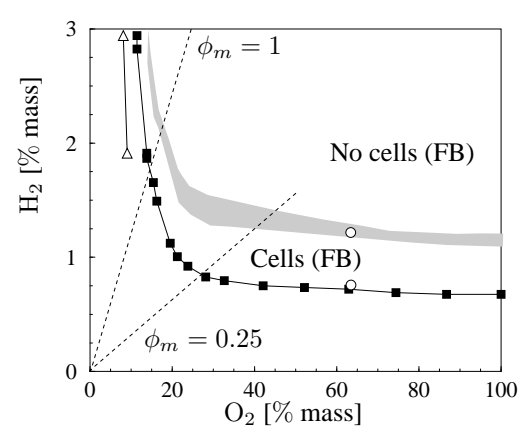
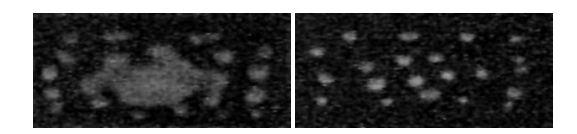


Figure 2. Near-extinction limits and region of cellular instability in nearly unstrained planar non-premixed  $CO_2$ -diluted  $H_2$ - $O_2$  flames; Shaded region: transition from non-cellular to cellular flames for the FB configuration; — $\blacksquare$ —: FB near-extinction limit; — $\Delta$ —: FT near-extinction limit;  $\circ$ : conditions for Fig. 3.



**Figure 3.** Digital images of the cells observed at the two points (o) in Fig. 2 for the FB configuration. Left: transition from no cells to the fully cellular regime; Right: near the extinction limit.

Next, the parameter space in which cellular flames are observed was determined for the FB configuration only. For the limited conditions examined to date in the FT configuration, no cells have been found yet. The transition region from a steady "featureless" flame to a flame with cells over its entire surface is identified in Fig. 2 by shading. Since the reactant Lewis numbers, based on the overall reactant mixture at 300 K, are relatively constant over the entire experimental range  $(0.97-1.33 \text{ for } O_2 \text{ and } 0.22-0.29 \text{ for } H_2)$ , Fig. 2 shows mainly the influence of Damköhler number (decreasing towards extinction) and initial mixture strength  $\phi_m$  on cell formation in the FB configuration (the experiments cover the range 0.05-3.55 and two lines of constant  $\phi_m$  are added in the figure for reference). Note that  $\phi_m$  is defined here as the ratio of the  $H_2$  and  $O_2$  mass fractions supplied in the fuel and oxidizer streams, respectively, normalized by the stoichiometric ratio. As in previous work [5], the distance in Fig. 2 between the appearance of cells and the extinction boundary increases with decreasing  $\phi_m$ . To illustrate the transition process to a fully cellular flame, Fig. 3 shows digital images taken for two conditions corresponding to the open circles in Fig. 2. They were taken with a movie camera at an oblique angle of about 45 degrees with respect to the vertical (cf. Fig. 1). About half way through the transition (left image of Fig. 3), cells have already formed on the periphery of the flame, while the center is still non-cellular. One possible explanation for this observation is the relatively larger heat loss of the flame edges to the chamber walls as compared to the flame center, i.e. a decrease of effective Damköhler number towards the flame edges. In the right image of Fig. 3 taken close to extinction, on the other hand, the entire flame consists of cells, which appear to be generated near the flame center and travel outwards before vanishing. The cell size at this point is smaller than at the transition, but still about 2 times the tube spacing.

Therefore, the cell size over the entire cellular regime appears to be unrelated to the spacing of the oxidizer supply tubes. Further towards extinction, the number of cells decreases progressively until the last cell "goes out".

## **OUTLOOK**

Theoretical studies [1, 2, 8] have shown that the reactant convected to the flame zone has a significant influence on the conditions for thermo-diffusive instabilities in non-premixed flames. When  $O_2$  diffuses against the bulk flow (our FB configuration), the current study and others (cf. [5]) have shown that cellular instabilities are more prevalent at low initial mixture strength and Lewis numbers, in agreement with theoretical predictions. In the opposite FT configuration, theory predicts that high initial mixture strength promotes cell formation. In addition, as opposed to the FB configuration, a low  $O_2$  Lewis number would be more important for cell formation than a low  $H_2$  Lewis number. The new burner, which has been shown to produce an essentially 1-D planar non-premixed flame with virtually no strain, appears to be well suited to test these theories. As mentioned above, no cells have so far been observed near the FT extinction limit in Fig. 2, despite the high  $\phi_m$ . The next step will therefore consist in lowering the oxidizer Lewis number and minimizing the effects of heat loss.

### References

- [1] S. Kukuck, M. Matalon, Combust. Theory Modeling 5 (2001) 217–240.
- [2] S. Cheatham, M. Matalon J. Fluid Mech. 414 (2000) 105–144.
- [3] J.S. Kim, Combust. Theory Modelling 1 (1997) 13-40.
- [4] R.-H. Chen, G.B. Mitchell, P.D. Ronney, Proc. Combust. Inst. 24 (1992) 213–221.
- [5] D. Lo Jacono, P. Papas, P.A. Monkewitz, Combust. Theory Modelling 7 (2003) 634-644.
- [6] M. Füri, Non-Premixed Jet Flame Instabilities, Ph.D. Thesis no. 2468, Swiss Federal Institute of Technology Lausanne (EPFL), (2001).
- [7] J. Du, R.L. Axelbaum, Proc. Combust. Inst. 26 (1996) 1137–1142.
- [8] V.N. Kurdyumov, M. Matalon, Proc. Combust. Inst. 29 (2002) 45–52.